Science and Technology of
Advanced Materials

Microstructures and fracture toughness of directionally solidified Mo–ZrC eutectic composites

To cite this article: Teppei Suzuki *et al* 2002 *Sci. Technol. Adv. Mater.* **3** 137

View the article online for updates and enhancements.

You may also like

- Fabrication, microstructure and properties of C/C-ZrC composites prepared by an asphalt-Zr(acac)$_4$ precursor
Wenqiang Lin, Si'an Chen, Yong Li et al.
- Novel nanocrystalline W–Cu–Cr–ZrC composite with ultra-high hardness
Lijun Cao, Chao Hou, Yurong Li et al.
- A first-principles study of the electronic, mechanical, vibrational, and optical properties of the zirconium carbide under high pressure
H Muñoz, J E Antonio, J M Cervantes et al.

This content was downloaded from IP address 3.149.238.159 on 21/05/2024 at 12:30

The STAM archive is now available from the IOP Publishing website http://www.iop.org/journals/STAM

ELSEVIER

Science and Technology of Advanced Materials 3 (2002) 137–143

SCIENCE AND TECHNOLOGY OF ADVANCED MATERIALS

www.elsevier.com/locate/stam

Microstructures and fracture toughness of directionally solidified Mo–ZrC eutectic composites

Teppei Suzuki*, Hiroaki Matsumoto[1], Naoyuki Nomura, Shuji Hanada

Institute for Materials Research, Tohoku University, 2-1-1, Katahira, Aoba-ku, Sendai 980-8577, Japan

Received 16 November 2001; revised 25 December 2001; accepted 25 December 2001

Abstract

Microstructures and fracture toughness of arc-melted and directionally solidified Mo–ZrC eutectic composites were investigated in this study. Two kinds of directionally solidified composites were prepared by spot-melting and floating zone-melting. Microstructure of the arc-melted composite (AMC) consists of equiaxed eutectic colonies, in which ZrC particles are dispersed. The spot-melted composite (SMC) exhibits spheroidal colony structure, which is rather inhomogeneous in size and morphology. ZrC fibers in the eutectic colonies are aligned almost parallel to the growth direction. Well aligned, homogeneous columnar structure with thin ZrC fibers evolves in the floating zone-melted composite (FZC). Texture measurement by X-ray diffractometry revealed that the growth direction of Mo solid solution (Mo_{SS}) in FZC is preferentially ⟨100⟩, while that of SMC is scattered. Fracture toughness K_Q evaluated by three point bending test using the single edge notched beam method is >13 MPa $m^{1/2}$ for AMC, 20 MPa $m^{1/2}$ for SMC and 9 MPa $m^{1/2}$ for FZC. Intergranular fracture along colony boundaries is often observed in AMC. In contrast, transgranular fracture is dominant in SMC and FZC, although significant gaps caused by intergranular fracture are occasionally observed in SEM micrographs of SMC. Fracture surface in FZC is wholly flat. Pull-out of ZrC occurs owing to Mo/ZrC interfacial debonding in intergranularly fractured regions of AMC and SMC.

Coarse elongated colonies in SMC and FZC induce transgranular fracture instead of intergranular fracture. Intergranular fracture and interfacial debonding in AMC and SMC causes frequent crack deflection accompanied by ligament formation and crack branching, which is responsible for the high fracture toughness of the composites. Preferred ⟨100⟩ growth of Mo_{SS} phase in FZC leads to brittle {100} cleavage fracture associated with low fracture toughness. © 2002 Elsevier Science Ltd. All rights reserved.

Keywords: Molybdenum; Zirconium carbide; Eutectic composite; Directional solidification; Fracture toughness; Fracture surface

1. Introduction

It is generally recognized in most structural materials that ductility and fracture toughness at ambient temperature are in conflict with strength at elevated temperature. Therefore, there have been many efforts to improve ductility and toughness of advanced intermetallics and refractory ceramics with high strength at elevated temperatures, which are candidates available for high temperature structural applications. Incorporating a second phase is one of the most effective techniques to improve the toughness without degradation of high temperature strength [1–3].

Recently, Mo–TiC, Mo–ZrC in-situ composites were investigated in light of harmonic materials design for high temperature structural materials [4–10], where Mo/TiC and Mo/ZrC systems have a eutectic reaction, thereby generating unique eutectic microstructure [4,7,11]. Kurishita et al. reported that strength of TiC could be enhanced by alloying with Mo [12]. As a result, these composites possess high strength at elevated temperature, which is comparable to that of the monolithic carbides [4,8]. In addition, since solubility of Ti, Zr and C is limited in Mo, ductility of Mo can be retained even in Mo solid solution (Mo_{SS}) of these in-situ composites [7,8]. According to Suzuki et al., owing to the contribution of Mo_{SS} as a ductile phase, hyper-eutectic composites exhibit fracture toughness K_Q of as high as 14–15 MPa $m^{1/2}$, even though they contain 44–52 vol% ZrC [8]. Eutectic composites are expected to show higher fracture toughness because of lower ZrC content. Additionally, microstructural control by directional solidification is available to improve the high temperature strength in the eutectic composite.

The present authors have previously applied directional solidification to Mo–16 mol%ZrC eutectic composite and obtained 10 mm long rods in the spot-melting method

* Corresponding author. Tel.: +81-22-215-2117; fax: +81-22-215-2116.
E-mail address: tsuzuki@imr.tohoku.ac.jp (T. Suzuki).
[1] Present address: Mitsui Mining and Smelting Corporation, 1333-2, Haraichi, Ageo, Saitama 362-0021, Japan.

1468-6996/02/$ - see front matter © 2002 Elsevier Science Ltd. All rights reserved.
PII: S1468-6996(02)00009-8

[9,10]. Compressive yield stress of the spot-melted composite (SMC) was found to be higher than that of the arc-melted composite (AMC) in the temperature range between 293 and 1773 K [10]. Yield strength of the SMC at 1773 K is as high as 418 MPa, which is higher than that of arc-melted Mo–30 mol%ZrC hyper-eutectic composite [8,10]. The floating zone (FZ) melting method is considered to be desirable to obtain much longer composite rods with homogeneous microstructure. However, we have never succeeded in growing Mo–16 mol%ZrC composite by FZ melting, because solid/liquid interface was so unstable in the process.

It is known that a slight deviation in composition from the eutectic point changes the phase stability in the ternary eutectic system [13]. For example, the slight deviation extends three-phase region of liquidus + Mo + ZrC, which causes unstable solid/liquid interface during the FZ-melting process [13]. The eutectic composition reported previously, Mo–16 mol%ZrC, was obtained from a study in the Mo/ZrC pseudo binary system [7]. More accurate analysis of the ternary eutectic composition would be required for microstructure control by FZ-melting. We have conducted the compositional analysis using an electron probe micro analyzer equipped with an image analyzer. The analysis indicated that the ternary eutectic composition is Mo–14.0 mol%Zr–11.7 mol%C.

We have developed multi-functional composites from the viewpoint of harmonic materials design for high temperature structural materials, where composites with multi-functions are designed without sacrificing the functional properties of components. In the present study microstructures and fracture toughness of Mo–ZrC eutectic composites are examined to obtain fundamental information for the toughness improvement. Two kinds of directionally solidified composites were prepared; one is spot-melted Mo–16 mol%ZrC and the other is FZ-melted Mo–14.0 mol%Zr–11.7 mol%C. Fracture toughness of the eutectic composites is discussed in relation to microstructural features.

2. Experimental procedure

2.1. Sample preparation

Nominal compositions of samples used in this study are Mo–16 mol%$ZrC_{0.94}$ (Mo–13.9 mol%Zr–13.2 mol%C) and Mo–14.0 mol%Zr–11.7 mol%C (compositions are given in mol% in this paper unless otherwise stated and abbreviated as Mo–16 ZrC and Mo–14.0Zr–11.7C, respectively). The raw material powders of molybdenum (99.98 mass% Mo) and zirconium carbide (99.4 mass% $ZrC_{0.94}$) were weighed at Mo–16ZrC and mixed in a cross-rotary blending machine for 18 ks. Then, the mixed powder was cold-pressed at room temperature. Commercial bulk materials of molybdenum (99.9 mass% Mo), zirconium (99.8 mass% Zr) and carbon (99.9 mass% C) were weighed at Mo–14.0Zr–11.7C. From each of raw materials, ingot bars of 100 mm long were obtained by arc-melting in an Ar gas atmosphere. The bars were roughly machined into 8 mm in diameter using an electro-discharge machine (EDM). Two kinds of directionally solidified composites were prepared by different processes as described later. One is by spot-melting method; the bar of Mo–16ZrC was melted by high frequency inductive heating in an Ar gas atmosphere and was not traveled but fixed on the same position. After stabilizing the melting zone, heating power was rapidly shut off. Then the solid/liquid interface moved up and down from the edge of the melting zone along the longitudinal direction of the bar. Thickness of melted zone was limited about 10 mm, which corresponds to directionally solidified zone in this process. The other directionally solidified composite of Mo–14.0Zr–11.7C was prepared by the conventional FZ-melting method; the bar was melted by inductive heating and traveled at 90 mm/min in an Ar gas atmosphere. Melting temperature of the composites prepared by the above processes was measured to be approximately 2800 K by an infrared radiation thermometer.

Samples were annealed at 1873 K for 252 ks in a vacuum of better than 3.0×10^{-3} Pa. Microstructure was examined by optical microscopy (OM) and scanning electron microscopy (SEM). Phase identification was performed by X-ray diffractometry (XRD) in conventional theta–2theta scanning. Texture measurement was carried out using XRD to investigate preferred growth direction of component phases in a directionally solidified composite.

2.2. Fracture toughness measurements

In order to evaluate fracture toughness, three point bending test using the single edge notched beam (SENB) method was conducted with reference to ASTM E399-90 and some reports [14–16]. A rectangular specimen was prepared by EDM in the dimension of $3 \times 6 \times 30$ mm^3. For SMC, melted part was put in the center of specimen. Surface of a specimen was polished by SiC paper. A blunt notch was introduced in the center of specimen to 3.0 mm in depth by EDM with a 0.10 mm diameter wire. The notch was introduced perpendicular to the growth direction in directionally solidified composites. The specimen was loaded at a cross-head speed of 0.5 mm/h on a 24 mm span in air at room temperature. From three point bending test using the SENB method, fracture toughness K_Q was estimated by the following equation [14,15]

$$K_Q = (P_Q S/BW^{3/2})\zeta$$

$$\zeta = \frac{3(a/W)^{1/2}[1.99 - (a/W)(1 - a/W)(2.15 - 3.93a/W + 2.7a^2/W^2)]}{2(1 + 2a/W)(1 - a/W)^{3/2}}$$

where P_Q is critical load, a is notch length, S is loading span and B and W are thickness and width of specimen, respectively.

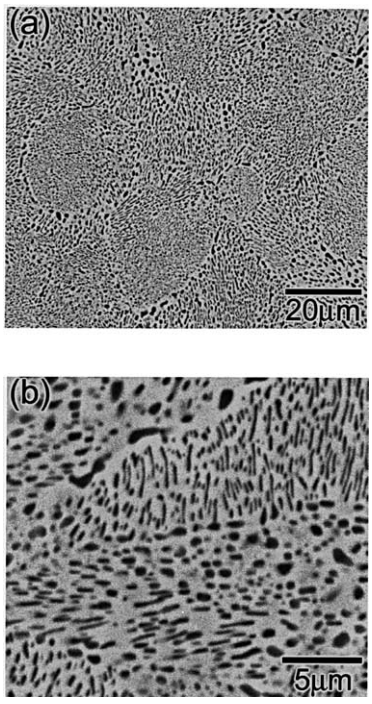

Fig. 1. SEM micrograph of arc melted Mo–14.0Zr–11.7C composite (AMC), (a) low magnification and (b) high magnification.

After bending test, fracture surface of each sample was observed by SEM.

3. Results

3.1. Microstructures

Microstructure of arc-melted Mo–14.0Zr–11.7C (AMC) after annealing at 1873 K for 252 ks is presented in Fig. 1. AMC exhibits typical eutectic microstructure containing equiaxed eutectic colonies with mean diameter of about 24 μm, as shown in Fig. 1(a). XRD analysis revealed that the composite consists of Mo_{SS} phase with A2 structure and ZrC phase with B1 structure. As seen in Fig. 1(a) and (b), fine ZrC particles are dispersed in Mo_{SS} and coarsened and/or fibrous ZrC particles are observed near colony boundaries. SEM observation shows that mean diameter of ZrC particles is about 400 nm and the volume fraction of ZrC phase is approximately 0.26. Microstructure of AMC is almost the same as that of arc-melted Mo–16ZrC [7].

Directionally solidified bar of about 10 mm long was obtained by spot-melting. Fig. 2(a) shows OM micrograph of SMC in the section parallel to the growth direction (longitudinal section). SMC consists of eutectic colonies elongated along the growth direction, and colony size and morphology is somewhat inhomogeneous. Fig. 2(b) is SEM micrograph of SMC in the longitudinal section, where ZrC fibers are aligned almost parallel to the growth direction. ZrC fibers are discontinuous and coarsened at colony boundaries, which is analogous to those in AMC. Fig. 2(c) shows microstructure of SMC in the section normal to the growth direction (transverse section). Equiaxed eutectic colonies are observed in this figure. This microstructure is quite similar to that of AMC. The observation in the two sections indicates that eutectic colonies of SMC have spheroidal shapes, which are elongated along the growth direction and somewhat inhomogeneous. Mean size of the colonies is about 430 μm in major axis and 140 μm in minor axis.

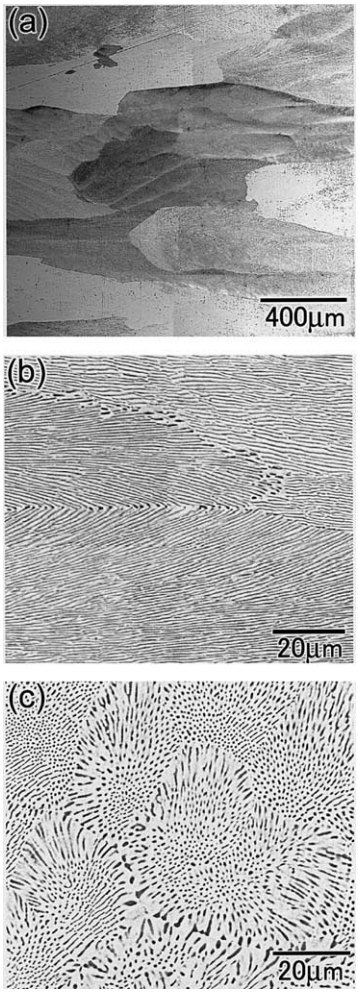

Fig. 2. Microstructure of spot-melted Mo–16ZrC composite (SMC) after annealing, (a) OM micrograph of a longitudinal section, (b) SEM micrograph of a longitudinal section and (c) SEM micrograph of a transverse section. The growth direction in (a) and (b) is horizontal.

Fine Mo–14.0Zr–11.7C composite bar with length greater than 60 mm was successfully fabricated by FZ-melting at a growth rate of 90 mm/h. Fig. 3(a) and (b) are micrographs of a longitudinal section in FZ-melted composite (FZC) after annealing. As is seen in Fig. 3(a), FZC consists of long, homogeneously elongated colonies, as compared with those of SMC. ZrC fibers aligned almost parallel to the growth direction are observed in Fig. 3(b). ZrC fibers in FZC appear to be thinner than those in SMC. The

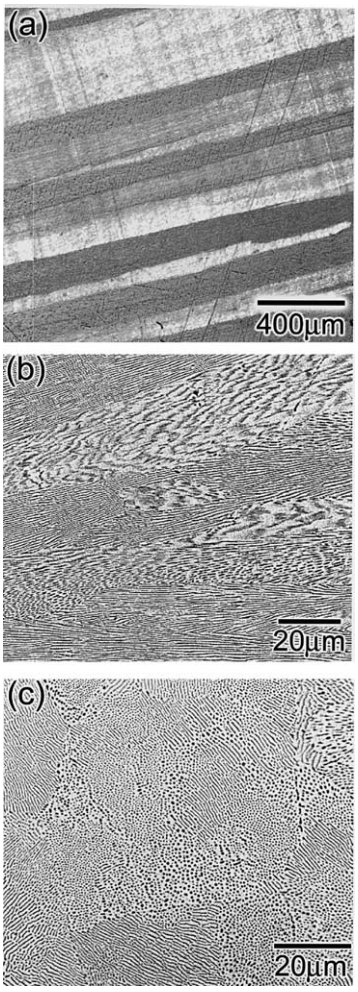

Fig. 3. Microstructure of FZ-melted Mo–14.0Zr–11.7C composite (FZC) after annealing, (a) OM micrograph of a longitudinal section, (b) SEM micrograph of a longitudinal section and (c) SEM micrograph of a transverse section. The growth direction in (a) and (b) is horizontal.

microstructure observed in a transverse section of FZC is presented in Fig. 3(c). This figure shows equiaxed colonies, which are similar to those of AMC and SMC. Consequently, FZC has columnar colony structure elongated along the growth direction. Most of the colonies in FZC are over 1000 μm long and mean length of minor axis is about 130 μm.

Texture measurement by XRD was conducted on SMC and FZC to identify the preferred orientation distribution of directionally solidified composites. Fig. 4 shows pole figures obtained from Mo_{SS} phase. No result of ZrC is presented here because of insufficient intensity ratio. Since the measurements were carried out on the transverse section of directionally solidified samples, normal direction (ND) in this figure corresponds to the growth direction. In FZC, significant accumulation at ND is found in (200) of Mo_{SS}, indicating that the preferred growth direction of Mo_{SS} in FZC is ⟨100⟩. On the other hand, although a tendency similar to FZC is seen in SMC, the orientation distribution is considerably scattered.

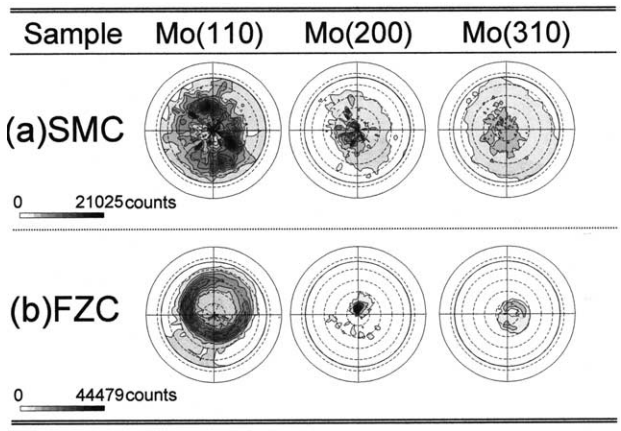

Fig. 4. Pole figures obtained by XRD texture measurement on the transverse section of (a) SMC and (b) FZC.

3.2. Fracture toughness

In order to evaluate fracture toughness of each composite, three point bending test in the SENB method was carried out at room temperature. Obtained load–displacement curves are presented in Fig. 5. AMC and SMC display non-linear behavior around a maximum load, indicating stable crack growth at an early stage of fracture. In contrast, FZC shows only linear behavior, which is probably due to absence of stable crack growth, i.e. catastrophic fracture.

Fracture toughness K_Q of each composite evaluated from the bending test is summarized in Table 1. Fracture toughness of arc-melted Mo–16ZrC is also included for comparison [9]. Evaluated fracture toughness value of AMC is almost the same as that of arc-melted Mo–16ZrC [9]. It should be noted that fracture toughness of FZC was as low as 9 MPa $m^{1/2}$, although that of SMC was over 20 MPa $m^{1/2}$.

3.3. Fracture surface

Fig. 6 shows SEM micrographs of fracture surface in AMC after bending test. From Fig. 6(a), it is found that

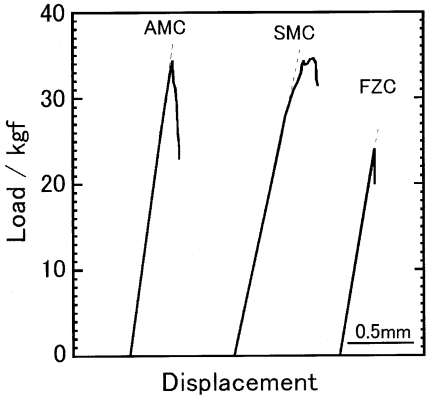

Fig. 5. Load–displacement curves of Mo–ZrC eutectic composites obtained by three point bending test at room temperature.

Table 1
Fracture toughness of Mo–ZrC eutectic composites obtained by three point bending test

Sample	Nominal composition (mol%)	Fracture toughness, K_Q (MPa $m^{1/2}$)	Area percentage of transgranular fracture, A_T	Size of eutectic colony, major axis, d_{maj}, and minor axis, d_{min} (μm)
Arc-melted Mo–16ZrC [9]	Mo–13.9Zr–13.2C	12.8	–	–
AMC	Mo–14.0Zr–11.7C	13.1	0.35	$d_{maj} \sim d_{min} = 23$
SMC	Mo–13.9Zr–13.2C	20.4	0.82	$d_{maj} = 480$, $d_{min} = 140$
FZC	Mo–14.0Zr–11.7C	9.4	~ 1	$d_{maj} = 2600$, $d_{min} = 120$

fracture surface of AMC is rough and complicated, suggesting that crack deflection occurs frequently. At a high magnification, intergranular fracture along eutectic colony boundaries is often observed in AMC, as shown in Fig. 6(b). Fig. 6(b) also exhibits pull-out of ZrC particle due to Mo/ZrC interfacial debonding. These two interfacial fractures in AMC result in complicated fracture surface.

Fig. 7 shows SEM micrographs of fracture surface in SMC. The fracture surface of Fig. 7(a) predominantly consists of relatively flat surface, as compared to that of AMC in Fig. 6(a). The surface involves river pattern, implying that transgranular cleavage fracture takes place. Using SEM image analyzer, the area percentage of transgranular fracture in fracture surface of SMC was measured as high as 82%, while that in AMC is 35%. Correspondingly, significant gaps due to intergranular fracture at colony boundaries were occasionally observed in SMC, as shown in Fig. 7(b). Pull-out of ZrC owing to Mo/ZrC interfacial debonding was also observed in the intergranular fracture region in a similar way to AMC.

Fracture surface of FZC after bending test is presented in Fig. 8. FZC exhibits wholly flat surface with river patterns. It is evident from Fig. 8(a) that the predominant fracture mode of FZC is transgranular cleavage. Fig. 8(b) is a high magnification micrograph of the fracture surface. This figure suggests that ZrC fibers are not resistant to the transgranular crack propagation.

4. Discussion

4.1. Fracture mode

Predominant fracture mode of Mo at room temperature is intergranular because of its intrinsic weakness of grain boundary [17,18]. In this case, a crack extends along weak grain boundaries almost parallel to a main crack plane.

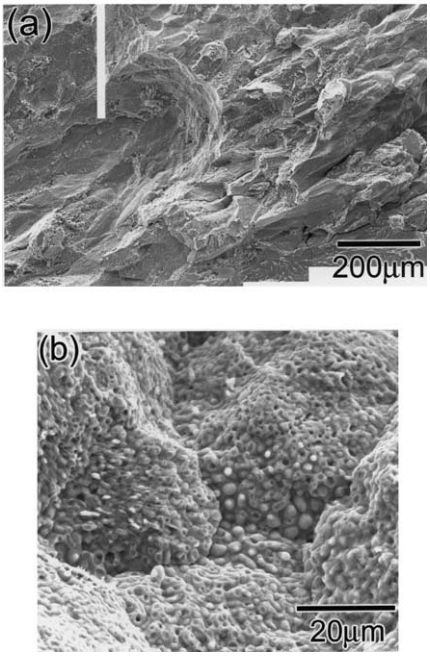

Fig. 6. Fracture surface of AMC composite after bending test, (a) low magnification and (b) high magnification in an intergranularly fractured region.

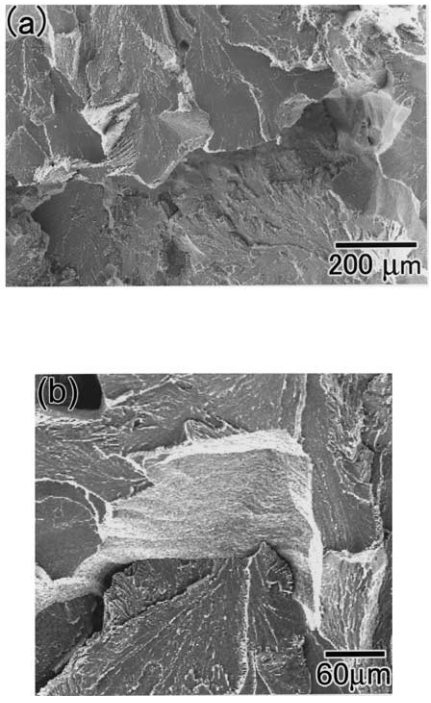

Fig. 7. Fracture surface of SMC composite after bending test, (a) low magnification and (b) a sharp gap caused by intergranular fracture.

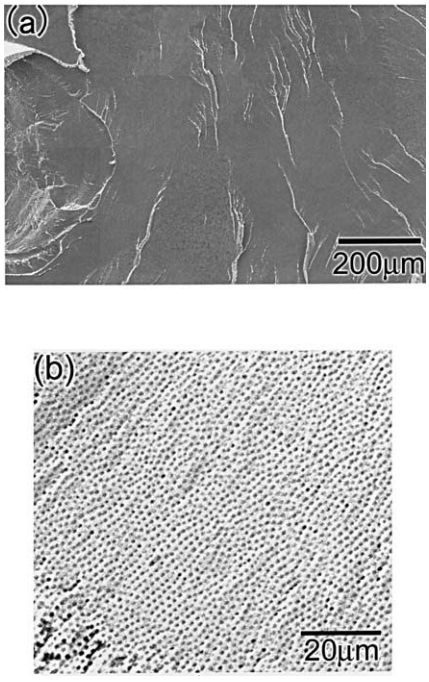

Fig. 8. Fracture surface of FZC composite after bending test, (a) low magnification and (b) high magnification.

Intergranular fracture along eutectic colonies was observed dominantly in AMC and occasionally in SMC. This intergranular fracture would attribute to the intrinsic weakness of grain boundary in Mo.

SMC and FZC exhibited transgranular fracture extensively. Both of the directionally solidified composites consist of coarse elongated eutectic colonies. Hiraoka and Hoshika [19] demonstrated that fracture mode of Mo alloy can be changed from intergranular to transgranular by evolving coarse elongated grain structure. It is suggested that such an inisotropic structure requires extremely high energy for intergranular fracture, since much larger surface area is necessarily generated. Thus, transgranular fracture is substituted for intergranular fracture when the aspect ratio and size of colony are increased in Mo alloy. Accordingly, intergranular fracture at colony boundaries is suppressed in the elongated colony structures like SMC and FZC.

In many alloys exhibiting grain boundary brittleness, e.g. Mo alloy, W alloy or some intermetallics, fracture toughness and deformability can be improved by suppressing intergranular fracture. Hiraoka and Hoshika succeeded in depressing ductile–brittle transition temperature of Mo alloy by developing coarse columnar microstructure [19]. According to their report, dominant fracture mode of Mo alloy with coarse columnar structure is transgranular [19]. Aoki et al. revealed that a small amount of B addition to Ni_3Al yields drastic change in the elongation by suppressing intergranular fracture [20].

In this study, AMC and SMC exhibit relatively high fracture toughness. Although the predominant fracture mode is changed from intergranular to transgranular by the formation of aligned colony structure, fracture toughness of FZC with the well-aligned microstructure is lower than that of AMC with the equiaxed colony structure. Correlation between fracture toughness and fracture mode of Mo–ZrC eutectic composite will be discussed in Section 4.2 and 4.3.

4.2. Intergranular fracture

Non-linear load–displacement behavior corresponding to stable crack growth is observed at an early stage of fracture in AMC and SMC. This behavior strongly suggests that some mechanisms such as crack bridging, crack branching, crack blunting with plastic deformation or shear ligament toughening are working for crack growth resistance. Fracture surfaces of AMC and SMC indicate crack deflection along colony boundaries. Particularly in SMC, significant gaps arising from intergranular fracture are occasionally observed. These gaps will be an indication of crack deflection in a large scale. It is most likely that the coarse colony size and spheroidal morphology is attributed to such crack deflection.

In addition, Mo/ZrC interfacial debonding is seen in the intergranularly fractured regions of AMC and SMC. The interfacial debonding also provides frequent crack deflection. It has been reported that frequent crack deflection, i.e. tilting and twisting, tends to generate unconnected crack path, which results in shear ligament toughening and/or crack branching [21]. Consequently, the crack deflection due to two kinds of interfacial fracture followed by ligament formation and/or crack branching would contribute to fracture toughness in AMC and SMC.

4.3. Transgranular fracture

Texture measurement of the growth direction in FZC revealed strongly preferred ⟨100⟩ orientation distribution of Mo_{SS} as shown in Fig. 4. In this study, a notch was introduced normal to the growth direction. Thus, the notch plane is parallel to {100} in FZC. In Mo single crystal {100} and {112} are known to be major cleavage planes, while {110} is to exhibit high fracture resistance [22]. Accordingly, brittle cleavage fracture and low fracture toughness in FZC would result from intrinsic brittleness along {100} of Mo_{SS}. On the other hand, orientation distributions of SMC is relatively scattered compared to FZC, as shown in Fig. 4. Such weak texture will suppress dominant {100} cleavage, thereby leading to partial intergranular fracture.

Consequently, the coarse columnar structure and preferred growth direction of $\langle 100 \rangle_{Mo}$ in FZC attribute to transgranular cleavage fracture and low fracture toughness. Crack deflection in a large scale due to local intergranular fracture would enhance the fracture toughness of SMC. The local intergranular fracture in SMC is concerned with its spheroidal colony morphology and weak texture along the growth direction of Mo_{SS}.

5. Summary

Microstructures and fracture toughness of arc-melted and directionally solidified Mo–ZrC eutectic composites were investigated in this study. Microstructure of AMC consists of equiaxed eutectic colonies, in which ZrC particles are dispersed. SMC exhibits rather inhomogeneous spheroidal colony structure. In colonies of the SMC, ZrC fibers are aligned almost parallel to the growth direction. Homogeneous columnar colony structure is observed in floating zone-melted composite (FZC). ZrC fibers in colonies are also aligned to the growth direction, and their thickness is smaller than that in the SMC. From XRD texture measurement, preferred growth direction of Mo_{SS} in the FZC is determined to be ⟨100⟩, while that of the SMC is not clearly identified because of considerable scattering of orientation.

Fracture toughness evaluated by three point bending test using the SENB method is 13 MPa $m^{1/2}$ for the AMC, 20 MPa $m^{1/2}$ for the SMC and 9 MPa $m^{1/2}$ for the FZC. Intergranular fracture along colony boundaries is predominantly observed in the AMC. On the contrary, the SMC exhibits dominant transgranular fracture. Significant gaps due to intergranular fracture are occasionally observed in the fracture surface of SMC. Pull-out of ZrC with Mo/ZrC interfacial debonding is seen on intergranular fracture surface of the two composites. Predominant transgranular fracture is observed in the FZC. Coarse elongated colony structure in the directionally solidified composites facilitates transgranular fracture instead of intergranular fracture.

It is concluded that crack deflection owing to intergranular fracture and Mo/ZrC interfacial debonding is responsible for the improved fracture toughness in AMC and SMC. Preferred growth direction of Mo_{SS} phase in the FZC induces {100} brittle cleavage fracture and results in low fracture toughness.

Acknowledgements

The authors would like to thank Mr S. Watanabe and Mr Y. Murakami for their technical assistance. We also acknowledge Mr I. Gunjishima for his assistance in directional solidification. This research was supported by a Grant-in-Aid for Scientific Research on Priority Area (No. 11221202) from the Ministry of Education, Science and Culture of Japan.

References

[1] A.G. Evans, High toughness ceramics, Mater. Sci. Engng A105/106 (1988) 65–75.
[2] M. Taya, Strengthening mechanism of metal matrix composite, Mater. Trans., JIM 32 (1991) 1–19.
[3] K.S. Chan, Fracture toughness of multiphase intermetallics, in: J. Horton, I. Baker, S. Hanada, R.D. Noebe, D.S. Schwartz (Eds.), Proceedings of the Symposium for the Materials Research Society, Materials Research Society, Pittsburgh, 1994, pp. 469–480.
[4] H. Kurishita, J. Shiraishi, R. Matsubara, H. Yoshinaga, Measurement, and analysis of the strength of Mo–TiC composites in the temperature range 285–2273 K, J. Jpn Inst. Met. 49 (1985) 963–971.
[5] N. Nomura, K. Yoshimi, T. Konno, S. Hanada, Fracture toughness improvement of TiC by Nb and Mo precipitates, J. Mater. Sci. Lett. 19 (2000) 1879–1881.
[6] T. Suzuki, N. Nomura, K. Yoshimi, S. Hanada, Microstructure and creep of Mo–ZrC in-situ composite, Mater. Trans., JIM 41 (2000) 1164–1167.
[7] T. Suzuki, H. Matsumoto, N. Nomura, K. Yoshimi, S. Hanada, Microstructures and mechanical properties of eutectic Mo–XC (X = Ti, Zr, Hf) in-situ composites, Trans. Mater. Res. Soc. Jpn 26 (2001) 307–310.
[8] T. Suzuki, N. Nomura, K. Yoshimi, S. Hanada, High-temperature strength and room-temperature fracture toughness of Mo–ZrC in-situ composites with hyper-eutectic structure, J. Jpn Inst. Met. 64 (2000) 1082–1088.
[9] T. Suzuki, H. Matsumoto, N. Nomura, N. Masahashi, S. Hanada, Microstructures and fracture toughness of Mo–ZrC eutectic composites, in: S. Hanada, Z. Zhong, S.W. Nam, R.N. Wright (Eds.), Proceeding of Fourth Pacific Rim International Conference on Advanced Materials and Processing, (PRICM4), Japan Institute of Metals, Sendai, 2001, 2763-2766.
[10] H. Matsumoto, Master's Thesis, Tohoku University, Sendai, Japan, 2001.
[11] P. Villars, A. Prince, H. Okamoto (Eds.), Handbook of Ternary Alloys Phase Diagrams, vol. 6, ASM International, Materials Park, OH, 1995, p. 7089, see also p. 7138.
[12] H. Kurishita, R. Matsubara, J. Shiraishi, H. Yoshinaga, Solution hardening of titanium carbide by molybdenum, J. Jpn Inst. Met. 53 (1985) 20–27.
[13] M. McLean, Directionally Solidified Materials for High Temperature Service, The Materials Society, London, 1983, pp. 79–86.
[14] Annual report of ASTM Standard, Standard Test Method for Plane-Strain Fracture Toughness of Metallic Materials, E399-90, ASTM, Philadelphia, 1997, pp. 408–438.
[15] J.R. Pickens, J. Gurland, The fracture toughness of WC–Co alloy measured on single-edge notched beam specimens precracked by electron discharge machining, Mater. Sci. Engng A33 (1978) 135–142.
[16] P. Ramasundaram, R. Bowman, W. Soboyejo, An investigation of fatigue and fracture in NiAl–Mo composites, Mater. Sci. Engng A248 (1998) 132–146.
[17] A. Kumar, B.L. Eyre, Grain boundary segregation and intergranular fracture in molybdenum, Proc. Soc. Lond A370 (1980) 431–458.
[18] J.B. Brosse, R. Fillit, M. Biscondi, Intrinsic intergranular brittleness of molybdenum, Scr. Metall. 15 (1981) 619–623.
[19] Y. Hiraoka, T. Hoshika, Parameter representing low-temperature fracture strength in molybdenum having an elongated and large grain structure, Int. J. Refr. Met. Hard Mater. 17 (1999) 339–344.
[20] K. Aoki, O. Izumi, Improvement in room temperature ductility of the $L1_2$ type intermetallic compound Ni_3Al by boron addition, J. Jpn Inst. Met. 43 (1979) 1190–1196.
[21] K.S. Chan, Micromechanics of shear ligament toughening, Met. Trans. A22 (1991) 2021–2029.
[22] K. Yoshimi, T. Suda, S. Hanada, submitted for publication.